CHAPTER 6

FLOW VISUALIZATION

6.1 Experimental Conditions and Procedure

In the present investigation, an experimental setup has been used for visualizing multi-phase flows in a vertical annulus flowing with water, Al_2O_3-water, TiO_2-water and SiO_2-water nanofluid with a concentration of 0.001%and 0.01% v/v to study the flow visualization during boiling heat transfer for low flow rate. The effect of supplied heat flux, mass flux and particle volume fraction on bubble behavior and flow regimes have been investigated**.** In first phase of experiments, alumina and titania nanofluids were used for the visualization. Flow patterns of water and nanofluids have been visualized and analyzed. Because of highly opaque nature of titania based nanofluid, bubble dynamics experiments have been conducted with alumina and silica nanofluid.

Obtaining images of flow boiling regimes was difficult and complicated by the presence of a large number of small bubbles. Transparent quartz cylinder has been fabricated for the test section to provide a view of the heating surface. High magnification with a well-adjusted focus and intense lighting were essential to capture and freeze the flow patterns and the coalescence of bubbles during flow boiling experiments. The transparent quartz cylinder provided optical accessibility enabling images to be taken from the camera on front side using reflected light from the illuminator on the back side. Present work employed two types of camera, first one (Nikon D5200 single lens reflex camera) to capture the flow patterns and second one (Motion BLITZ Cube High Speed Camera, manufactured by Mikrotron GmbH) to capture the bubble behavior of water and nanofluids. The high-speed video camera was adjusted to focus on nucleating bubbles. In

order to capture the very short bubble growth phenomenon, the frame rate was set at 1000 frames/s with a resolution of 1280 × 1024 pixels. For each recording, a total of 12,000 frames of images were taken by the high speed camera and downloaded to a computer. Recordings for each experimental condition were made 2–3 times to ensure the repeatability of the results. The bubble images obtained by the high speed camera were downloaded to the computer and analyzed using image processing software ImageJ to measure the bubble characteristics for the present experiments.

6.2 Flow patterns of water and nanofluids

High-speed visualization plays important role in flow boiling research to study very short-time phenomenon of bubble behavior. Figure 6.1 shows the visualization results of flow regimes of the flow boiling heat transfer, which consisted of convective heat transfer, nucleate boiling heat transfer and local dry out of heater rod in terms of single phase liquid, bubbly flow, dispersed bubbly flow, churn flow and dry patches on top section of the heater. In all the cases, liquid entered the test section at the bottom of the test section under subcooled condition at atmospheric pressure and heater wall temperature was below the saturation temperature. The flow of liquid direction is against the gravity. With the increasing applied heat flux, the bulk liquid temperature and the wall temperature varied along the length of the tube. In all the cases, the flow pattern has been initiated with single phase, fully developed and non-boiling regime as seen in Fig. 6.1 at applied heat flux of 32.2 kW/m^2. As the heat input is increased further, at 87.5 kW/m^2, the first bubbles appear on the wall being identified as the onset of nucleate boiling (ONB) in water. However, forced convective regime continued in case of 0.001% Al_2O_3-water nanofluid till the heat flux is increased up to 103.6 kW/m^2 whereas nucleate boiling regime prevails in case of water. The increase in single phase heat transfer performance is attributed to nanoparticle interaction with the heater wall and working fluid. The effective

conductivity of nanofluids increased by dispersion of suspended particles, intensification of turbulence and Brownian motion [142]. The nanoparticles act as heat carriers, collide with the heated surface, disturbing the boundary layer of bulk fluid. This phenomenon increases the temperature gradient near the wall which enhances heat transfer [143]. As the heat flux is increased further, at 103.6 kW/m^2, partial boiling appeared in water and nucleation began in 0.001% Al_2O_3-water nanofluid and 0.001% TiO_2-water nanofluid, showing ONB. The reason may be attributed to the presence of nanoparticles which filled the cavities on the heater surface due to enhanced wettability and required higher wall superheat for initiation of boiling. However, 0.01% Al_2O_3-water nanofluid exhibited earlier ONB than water due to higher concentration of nanoparticles which were responsible for the surface modification during boiling. The deposition of nanoparticles on the heater surface increased active nucleation site density and initiated the nucleate boiling at a lower heat flux. Another reason may be that viscosity increases with increase in particle concentration and plays a dominant role in turbulent flow, thus influencing the flow boiling heat transfer. Visual images of 0.01% TiO_2-water nanofluid has not been produced in this study because of its highly opaque nature.

As the wall superheat is increased further, different flow patterns were observed with increasing heat flux. In case of water, small discrete bubbles appeared in bubbly flow at a heat flux of 127.3 kW/m^2 which developed into larger coalesced bubbles changing the flow pattern to churn flow and eventually dry patches appeared on the heater rod exhibiting departure from nucleate boiling (DNB) at 167.5 kW/m^2. However, in case of nanofluid flow boiling, discrete bubbles were observed and the flow pattern became dispersed bubbly flow. The delay in DNB was quite significant with increase in concentration. The local dryout phenomenon occurred at 202.7 kW/m^2 for 0.001% Al_2O_3-waternanofluid and at 235.3 kW/m^2 for 0.01% Al_2O_3-water nanofluid. So, it was clear

from the flow regimes that DNB was delayed in nanofluid flow boiling as compared to pure water.

During flow boiling experiments using water, small bubbles were observed initially on the heater wall indicating onset of nucleate boiling (ONB). As the heat flux was increased, nucleate boiling (NB) phenomenon progressed quickly and bubbles coalesced to form larger bubbles which indicated departure from nucleate boiling (DNB). Subsequently, churn flow was witnessed with fluid traversing up and down in oscillatory manner with an aggregate upward flow. Churn flow caused the test section to vibrate and also dry patches started to develop on the heater surface in the top part. At this instant, power to the heater was cut-off to avoid burnout of the heater rod.

However, during experimentation with Al_2O_3-water and TiO_2-waternanofluids, bubbles do not coalesce easily and discrete bubble regime endures for a longer time even though heat flux was increased. Thus experiments suggest that heater surface is continuously modified morphologically during nanofluid flow boiling, making nanofluid boiling performance dependent on applied heat flux and particle concentration. The nanoparticle deposition on the heater caused by microlayer evaporation keeps modifying the heater surface and alter the boiling phenomenon. This phenomenon is predominant at higher heat fluxes which causes delayed flow regime resulting from the wettability enhancement due to nanoparticle deposition.

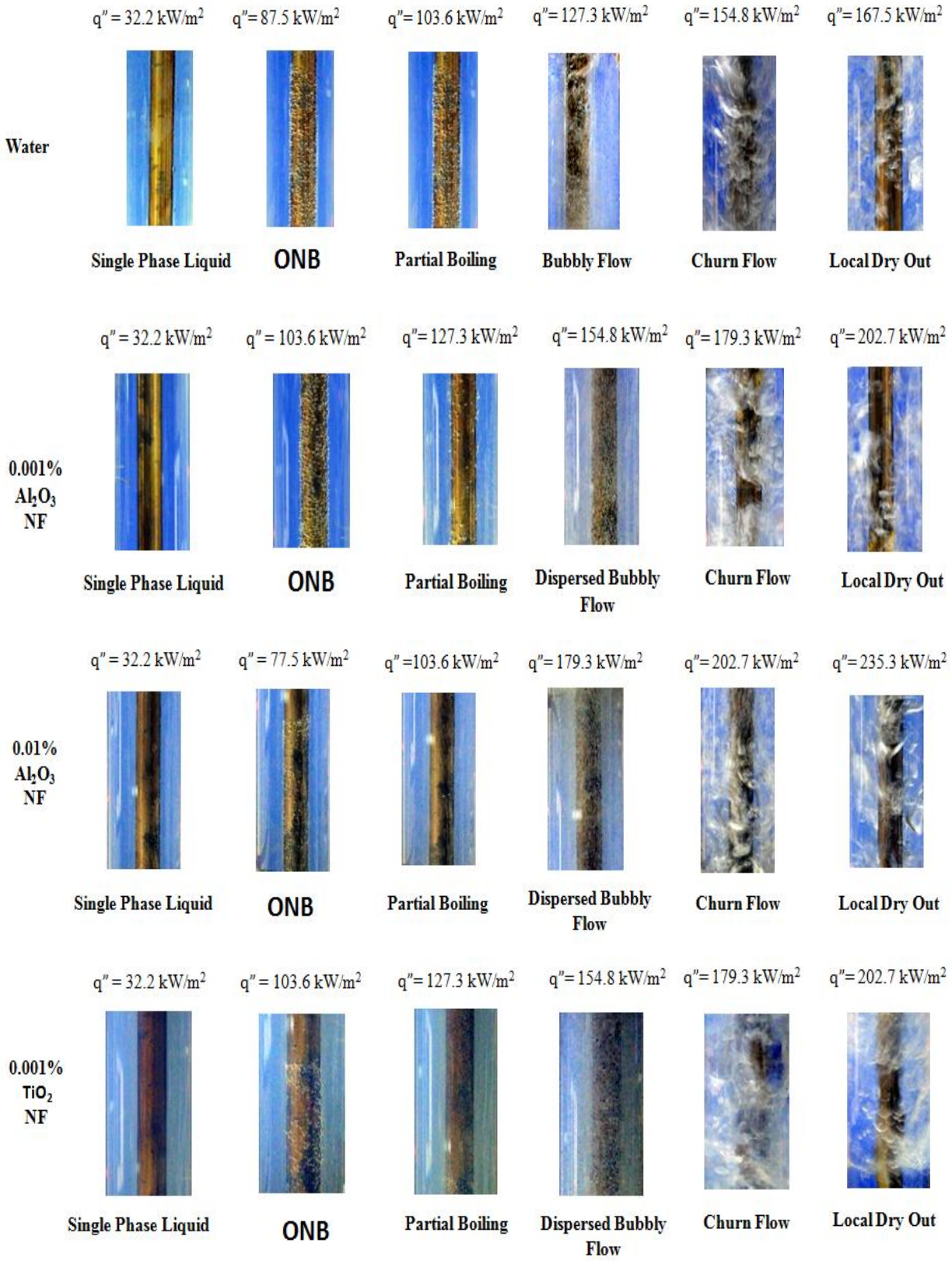

Fig. 6.1 Flow patterns of water and water based nanofluids at different heat fluxes at a mass flux of 6 kg/m^{2}s

6.3. Bubble Dynamics

The detailed physics of bubble growth is very complex, and occur on very small length scales in the vicinity of the heater surface. The heat transfer at the solid-liquid interface is highly influenced by the bubble dynamics which includes nucleation, growth and departure of bubbles. The bubbles remove large quantities of heat from the heated surface at relatively low surface temperatures. The estimation of evaporative and quenching heat transfer in Rensselaer Polytechnic Institute (RPI) wall boiling model of Kurul and Podowski [144] requires the information of various bubble departure characteristics. Visualization of the liquid–vapor phase and bubble dynamics may contribute greatly to our understanding of the characteristics of nucleate boiling heat transfer.

The bubble behavior observed in the present experiments could be classified into the following two types: (a) bubble nucleation and growth on the heated surface (b) bubble liftoff from the heated surface. The bubble behaviour of a water bubble at a heat flux of 61.5 kW/m^2 is depicted in Fig. 6.2. It is observed that bubbles nucleate on the heater surface, grow while sliding and finally get lifted off from the surface and condense in the main stream.

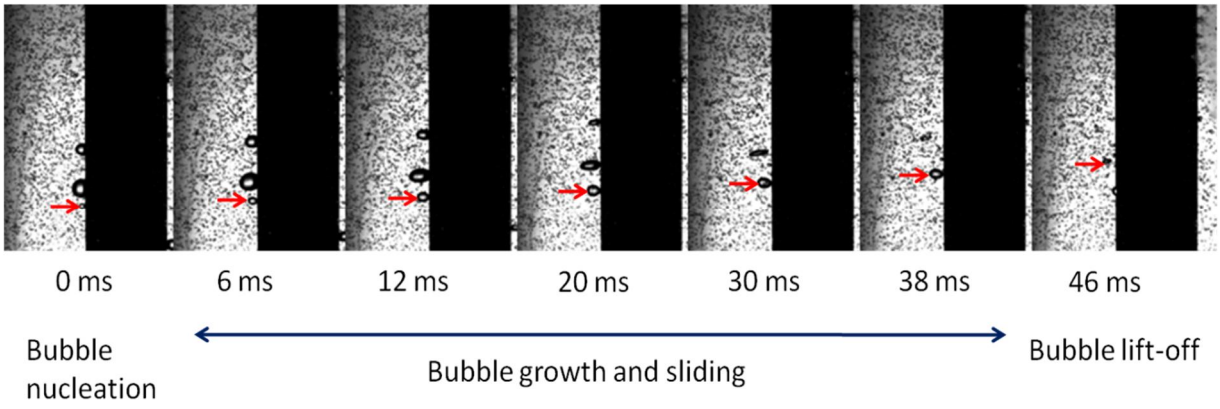

Fig. 6.2 Bubble behaviour of a water bubble (ΔT_{sub} = 20 K, $\dot{m}$ = 12 kg/m^{2}s)

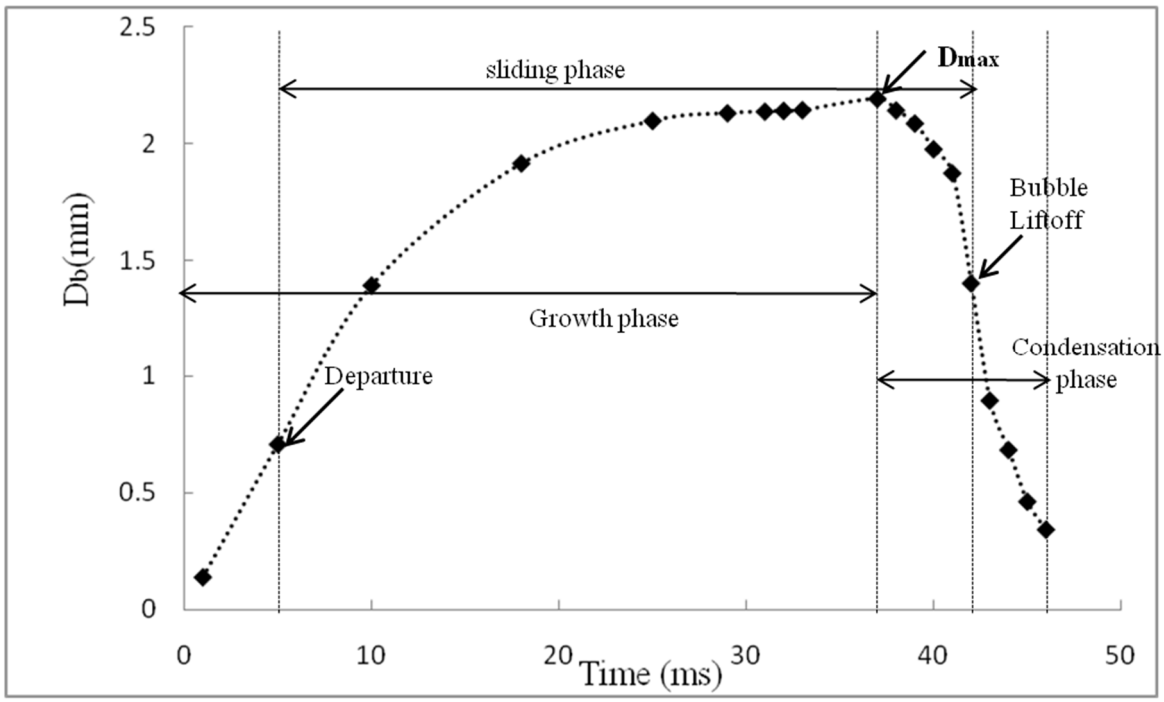

Fig. 6.3 Bubble growth curve of water bubble (ΔT_{sub} = 20 K, $\dot{m} = 12$ kg/m^{2}s)

During the bubble growth, bubbles grow to achieve a maximum size till the rate of evaporation equates the rate of condensation. After this point, condensation dominates and bubble starts shrinking which leads to bubble lift-off. Figure 6.3 exhibits the bubble growth curve of a water bubble. The growth curve of bubble has been obtained by measuring the diameter of an individual bubble from incipience through sliding. After some time, the bubble leaves the heater surface and gets ejected into the bulk liquid where it condenses completely. Variation of the bubble diameter during the bubble growth time has been plotted in the graph. Figure 6.4 demonstrates the growth curves of various bubbles nucleating from the same nucleation site under identical conditions. It can be seen that the growth rates are almost identical for all the bubbles nucleating under identical conditions with slight variation in maximum bubble diameter and bubble lifetime.

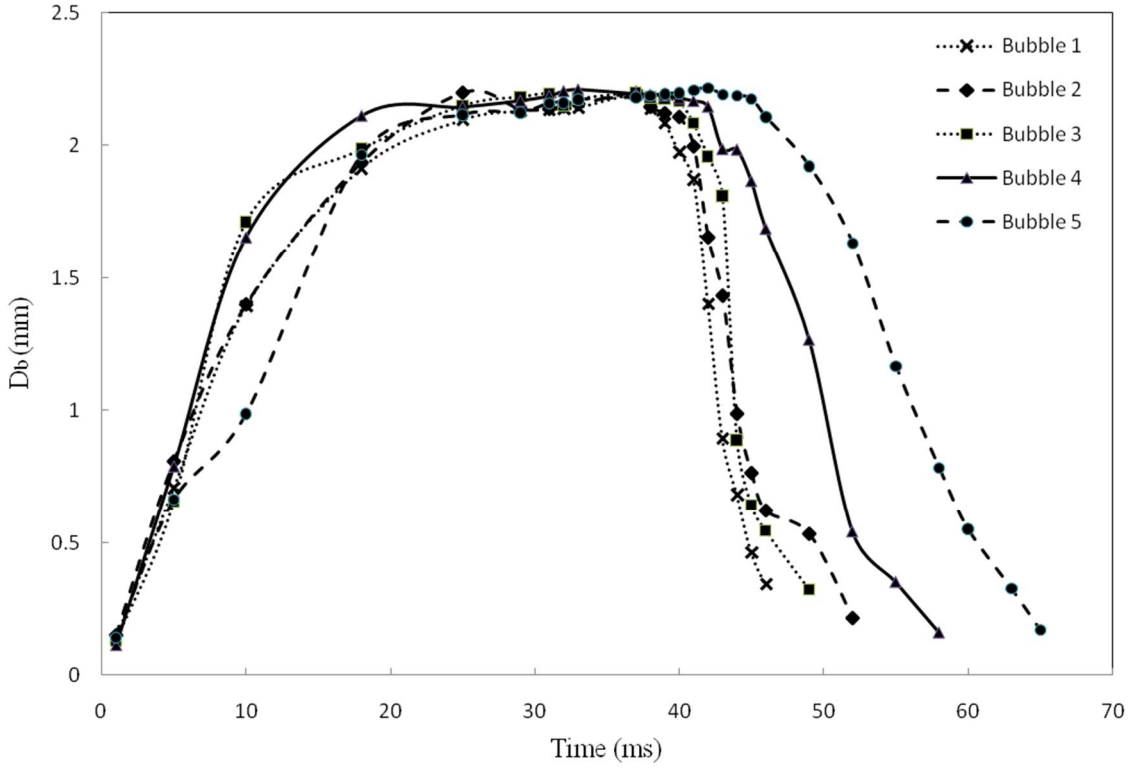

Fig. 6.4 Bubble growth curves for various water bubbles (ΔT_{sub} = 20 K, $\dot{m}$ = 12 kg/m^{2}s)

The bubble diameters and frequencies were measured using the high-speed images. For each experimental case, few nucleating sites were selected. The bubbles departing from these sites were then observed for the bubble departure characteristics. All this aspects of bubble dynamics have been studied in detail and the results of water and nanofluids have been compared

6.3.1. Observation of Bubble Structure

Figure 6.5 depicts the bubble structure at varying heat flux conditions in this study. Bubble images captured by high speed camera show the bubble behavior during flow boiling of water and nanofluid at various heat fluxes. In general, when the heater surface exceeds the saturation temperature of the bulk fluid, bubbles are nucleated on the heater surface and get departed in the upward direction. Initially few individual sites develop at lower heat flux and consequently the site density and the bubble size increase

as the heat flux is increased. The results demonstrate increasing bubble population for both water and nanofluid with increased heat flux. The reason may be attributed to increased value of wall super heat which leads to increase in the number of nucleation sites. Actually the heating surface has micro cavities which are filled with a pre-existing region of inert gases and vapor and these cavities act as nucleation sites at low wall superheat. At low heat flux (61.5, 71.66 kW/m^2), less number of isolated bubbles were formed on the heater surface at the point of ONB. Hence, in this region, bubbles grew individually and were almost not influenced by the neighboring bubbles. However, with increasing heat flux, bubbles from neighboring nucleation sites collide and coalesce and form large irregular bubbles. The phenomenon of collision and coalescence occurs more frequently at higher heat fluxes making the flow bubbly and chaotic. This phenomenon is predominant in pure water and the bubble size is larger causing flow disturbance at higher heat flux ($\sim$130 kW/m^2).

However, during experimentation with Al_2O_3-water and SiO_2-water nanofluids, bubbles do not coalesce easily and discrete bubble regime endures for a longer time even though heat flux was increased. At higher heat flux, nanoparticles plug in nucleation cavities and deactivate the cavities in the presence of highly wetting liquid, which leads to decrease in the bubble population. Due to higher wettability of nanofluids compared with base fluid, the cavities on the heating surface get filled by the nanofluid and become inactive or flooded, which results in increased value of wall superheat required for initiation of nanofluid boiling [40].

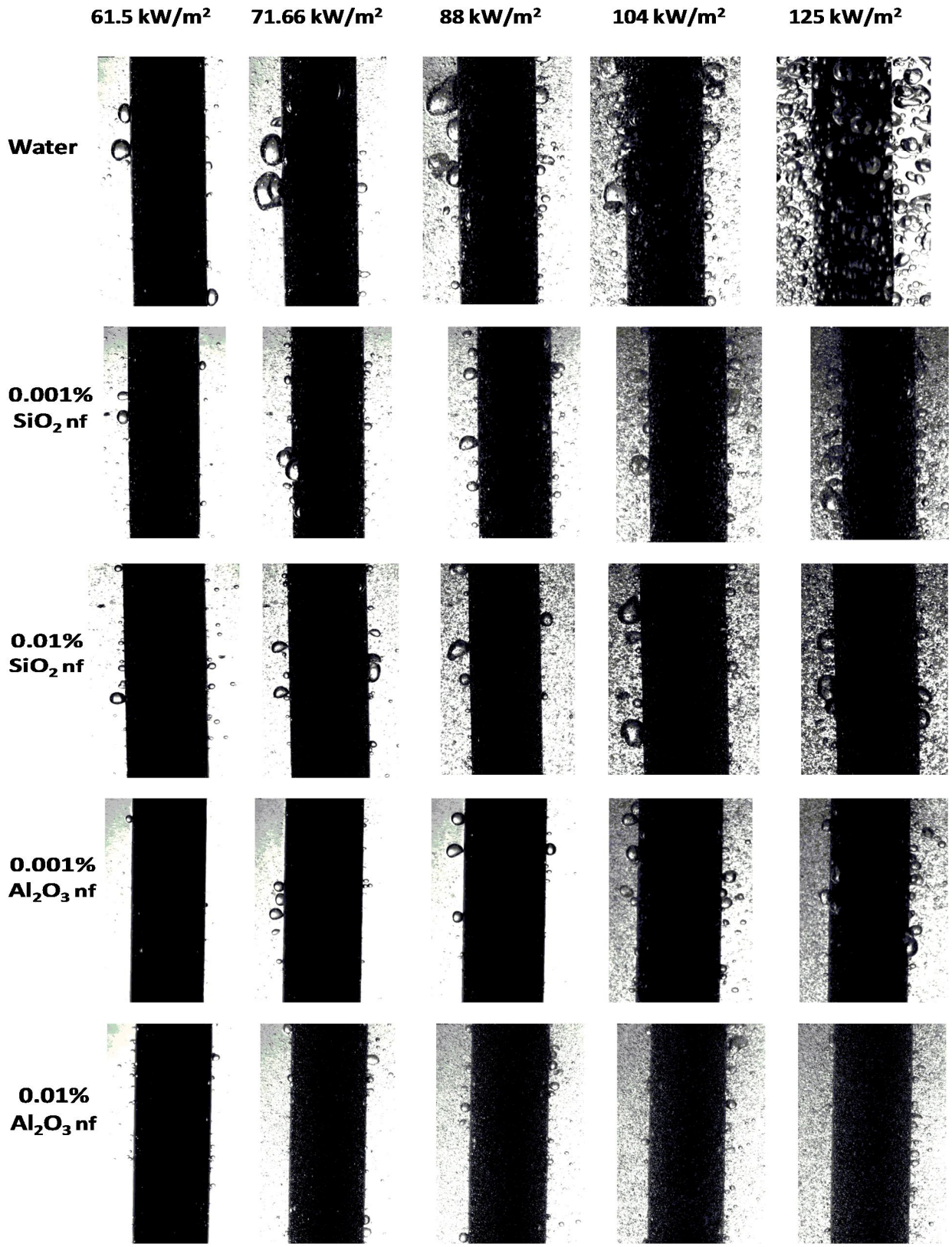

Fig. 6.5 Bubble Structure observation of water and nanofluids

(ΔT_{sub}= 20 K, mass flux= 3.8 kg/m^{2}s)

6.3.2 Bubble Nucleation and growth at varying heat flux

During this study, the attention has been focused on a single nucleating bubble originating from the heater surface. The bubble grew at the nucleation site due to evaporation at the solid-liquid interface when the heater surface temperature goes beyond local saturation temperature of the flowing liquid. The bubble growth and nucleation is observed near onset of nucleate boiling at a heat flux of 61.5 kW/m^2 and near onset of significant void at 88.5 kW/m^2. After the initial growth, the typical bubble motion includes departure and subsequently detaching from the wall and then condensing into a smaller sized bubble.

Figure 6.6 represents consecutive images of bubble nucleation, sliding and departure in pure water and 0.01% of alumina, silica nanofluid at inlet temperature of 80°C, heat flux of 61.5 kW/m^2 and mass flux of 3.8 kg/m^2s. In order to capture the bubble growth which is a very short phenomenon, the high speed camera was adjusted to focus on an active nucleation site. As soon as small bubbles appeared on the heater surface indicating onset of nucleate boiling, high speed recordings were made to estimate the bubble characteristics. At ONB, bubble behavior was found to be almost identical for water as well as nanofluids, i.e. bubble nucleated and grew at the site, then started to slide while attached to the surface and lastly detached from the heater wall and gets ejected into the subcooled bulk liquid. As seen from the images, the bubbles in nanofluids are little bigger than in pure water indicating higher heat transfer at the solid-liquid interface. Similar results were observed in case of 0.001% concentration of both the nanofluids.

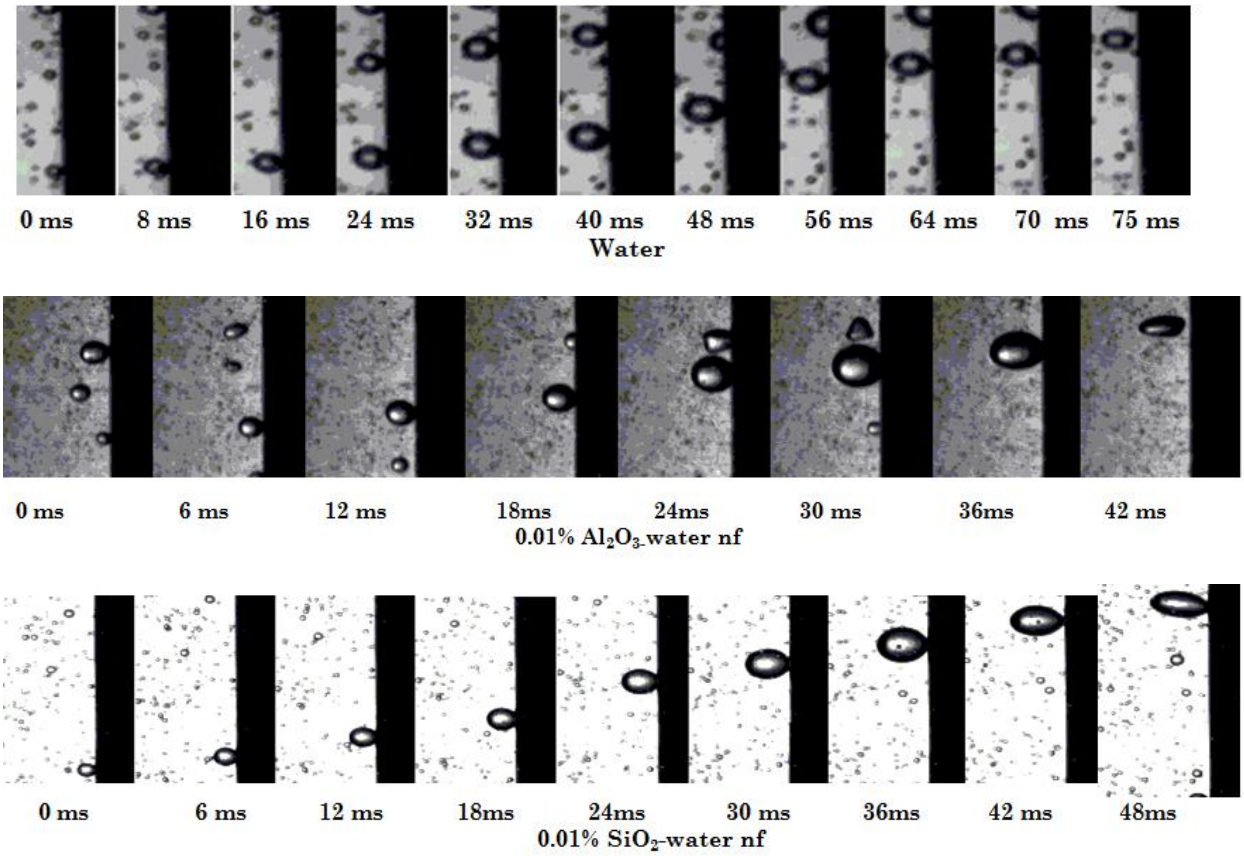

Fig. 6.6 Sequential images of bubble growth and lift-off at ONB

As heat flux is increased further, beyond 90 kW/m^2, the amount of vapor increased in the test section with larger bubbles nucleating on the heater surface. Because of higher heat flux, local subcooling decreases and the departed bubbles sustain in the main stream. This phenomenon increases the bubble volume as well as bubble population thereby increasing void fraction in the column indicating the commencement of onset of significant void (OSV). As heat flux increases, bubble size increases in water as well as nanofluids. However, bubble growth is more prominent in water than in nanofluids exhibiting bigger and flat bubbles. The bubble spreading is more in water covering a larger area of the heater surface as seen in Fig. 6.7. In pure water, bubbles were held for a longer time on the heater surface before lift-off. But with nanofluids, the bubbles were propelled into bulk liquid within a short period of time after detachment from the heater surface. Hence bubble life time was shortened in case of nanofluids as compared to pure

water and smaller, round bubbles were formed in nanofluids. The nanofluid boiling formed a porous nanolayer because of microlayer evaporation leaving behind nanoparticles glued to the heating surface [145]. The change in bubble behavior might be caused by the altered surface properties such as thermal resistance and surface roughness due to nanoparticle deposition during nanofluid boiling.

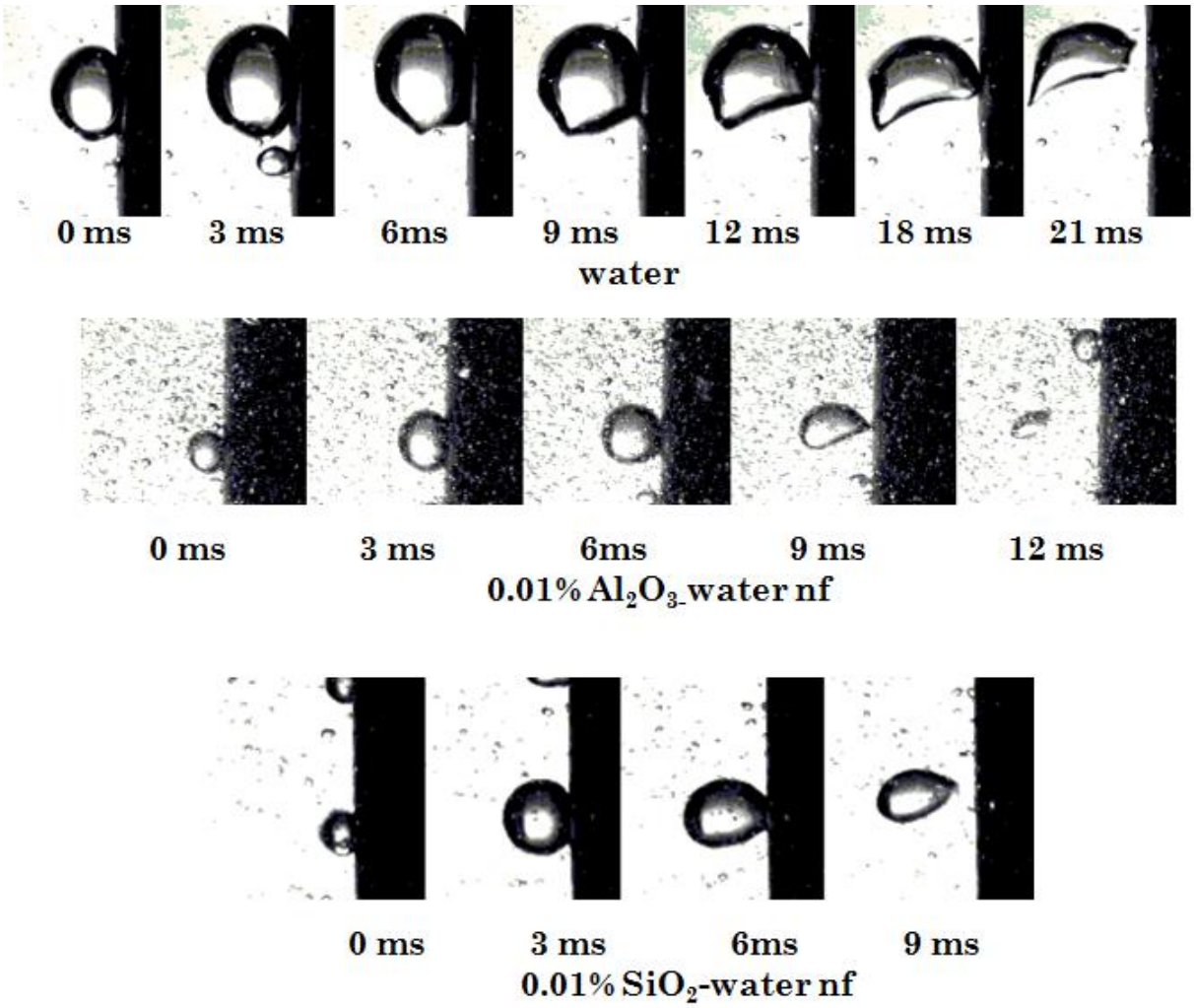

Fig. 6.7 Sequential images of bubble growth and lift-off at OSV

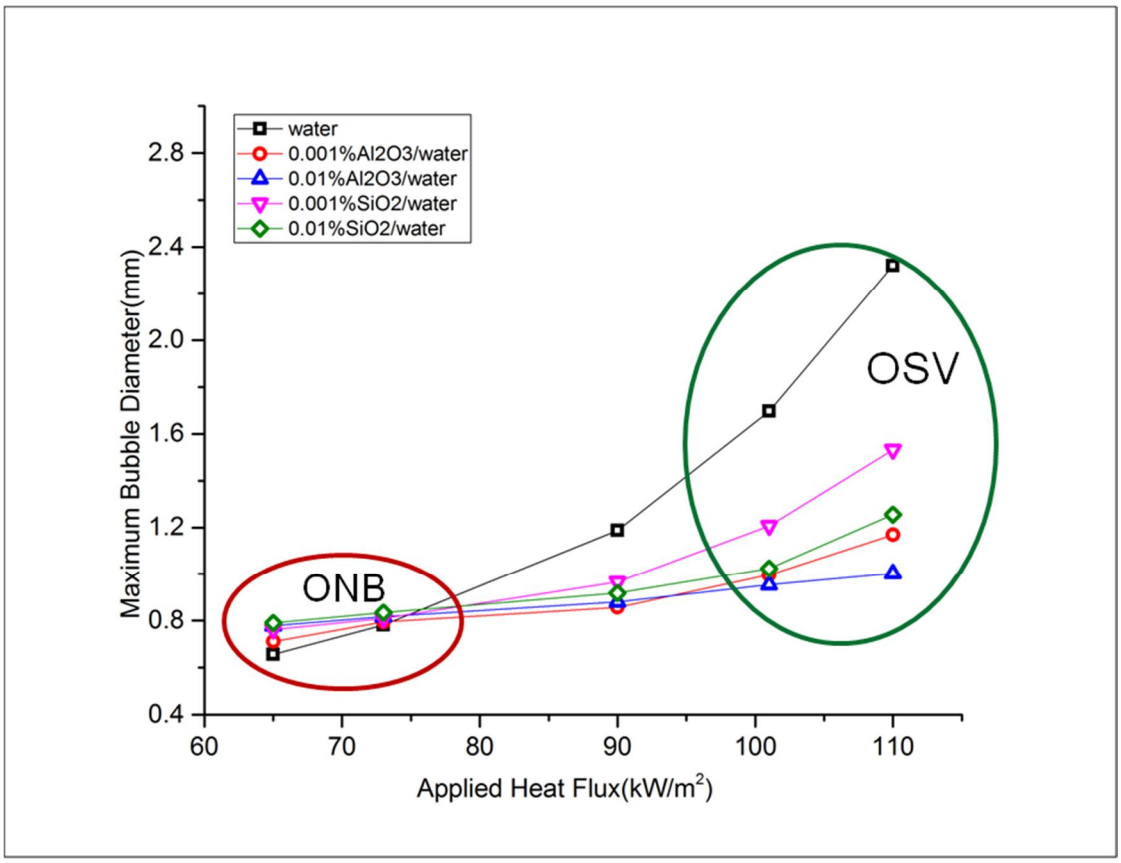

Fig. 6.8 Effect of heat flux and nanoparticle concentration on Maximum Bubble Diameter

The effect of heat flux and nanoparticle concentration on bubble diameter has been shown in Fig. 6.8. It is observed that bubble size increases with increase in heat flux for both water and nanofluids. Due to higher wall superheat at high heat flux, bigger bubbles were formed. At lower heat flux, near ONB (as marked in red circle), the bubbles are almost similar in water and nanofluids. But the pattern differs at higher heat flux near OSV (as marked in green circle). The bubble growth is high and very big bubbles are formed in water as shown in Fig. 6.7. However, bubble growth was less for 0.001% and 0.01% Al_2O_3/water as well as SiO_2/water nanofluids. The reason may be attributed to decreased surface tension force which is responsible for smaller bubbles in nanofluids [16]. Hence the contact area between heater surface and bubble decreases and inhibits the formation of dry patch.

Due to larger size of the bubble and greater bubble life time, the phenomenon of bubble coalescence was more frequent in water. This in turn produced large, irregular bubbles which changed the flow pattern from bubbly flow to churn flow much faster. The bubble coalescence phenomenon of water, 0.001% of Al_2O_3/water and SiO_2/water nanofluids at inlet subcooling of 20 K and mass flux of 3.8 kg/m^{2}s have been shown in Fig. 6.9. Because of greater bubble life time, bubble coalescence is also longer in case of pure water. This facilitates the merging of other sliding and nucleating bubbles and the flow becomes chaotic caused by random bubble coalescence. As observed in recordings, occurrence of bubble coalescence was less in nanofluids. Even if it happened, the duration was very short and thus produced smaller bubbles. The transition from bubbly flow to churn flow was slow and happened at a higher heat flux as shown in Fig. 6.13. The occurrence of bubble coalescence was rare in case of 0.01% volume fraction of both the nanofluids. The reason may be attributed to the departure size of the bubbles which was very small in case of higher concentration of nanofluids.

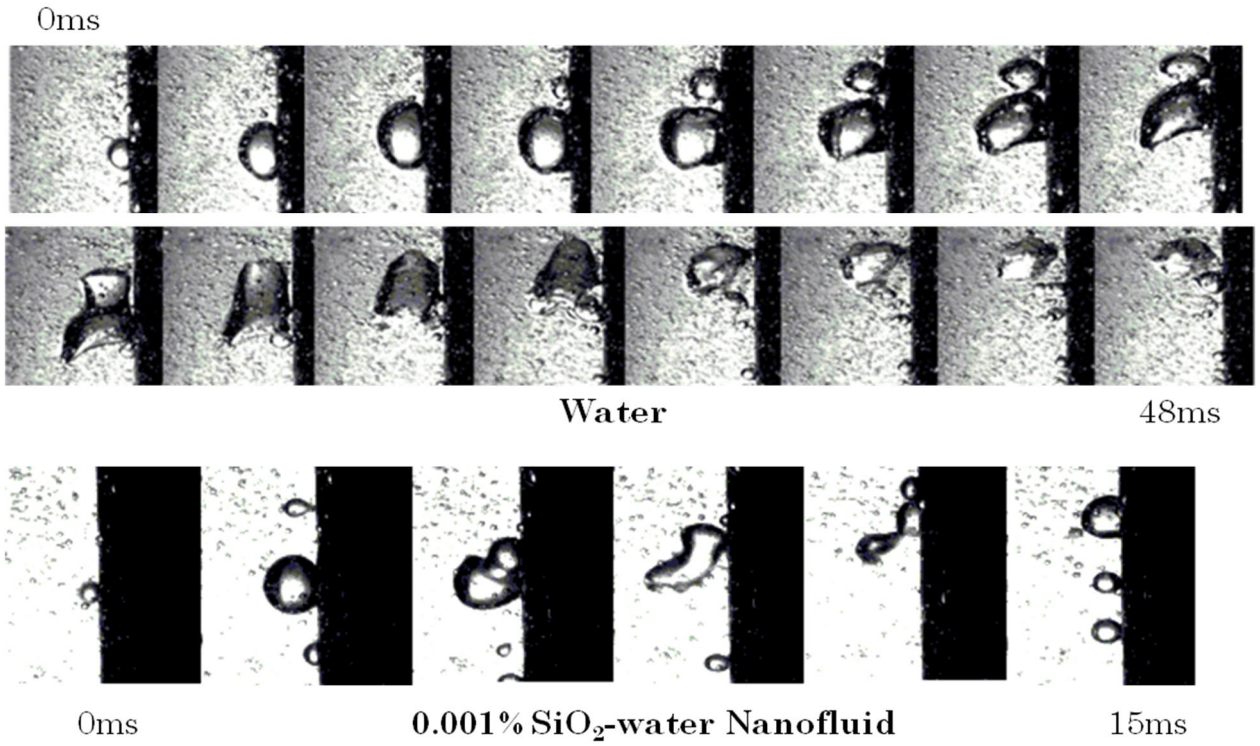

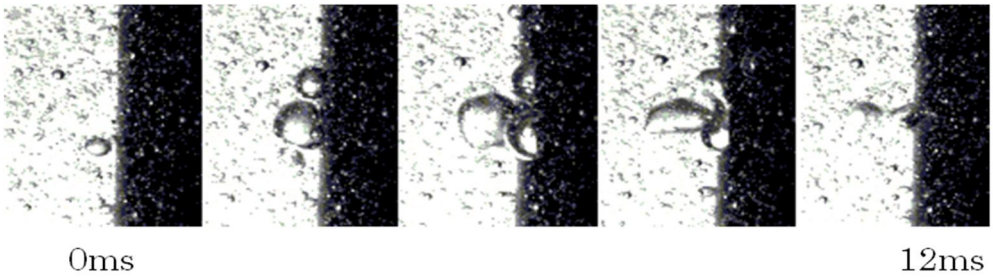

Fig. 6.9 Bubble Coalescence Phenomenon

6.3.3 Bubble Departure Characteristics

Irregular bubble growth causes irregular boiling heat transfer and flow instability. Hence, study on bubble growth and departure is of great importance to understand the boiling mechanism. After nucleation, bubbles adhered to nucleation sites for a certain time and then started to slide up the vertical heated surface as observed in the high speed visualization. During sliding, the bubble grew continuously through heat transfers from both superheated liquid layer at the surface and the microlayer beneath the bubbles. After sliding a certain distance, the bubble was detached from the wall and gets ejected into the subcooled bulk water flow. The bubble departure diameter is defined as the bubble diameter when the bubble just departs from the nucleation site. The detection of bubble departure was little difficult since the bubble stayed at the nucleation site for a very short period. High speed images were analyzed carefully to measure bubble departure diameter. The data of bubble departure diameter for water and nanofluids at different heat fluxes has been plotted in Fig. 6.10.

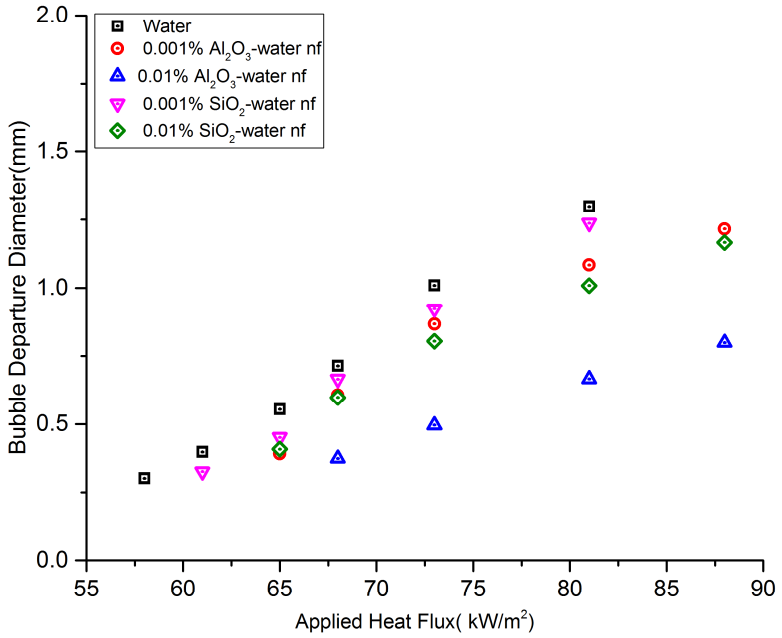

Fig. 6.10 Effect of heat flux on the bubble departure diameter

It is observed that bubble departure diameter increases with increase in heat flux for both water and nanofluids. The increase in heat flux causes increase in wall superheat, which results in a higher evaporative heat transfer producing larger bubbles. However, departure diameter decreases in nanofluids as compared to pure water. The addition of nanoparticles into the base fluid significantly changed the interfacial behaviour of the bubbles. This was supposed to be the major reason responsible for the distinctly changed two-phase flow characteristics (smaller bubble departure diameter) of nanofluid flow boiling than those of water flow boiling. Based on the classical bubble dynamics theory, the balance among the buoyancy force, surface tension force, drag force and inertia force controls the bubble growth and departure. The decreased surface tension force accounts for the miniature bubbles in nanofluid boiling [16]. Furthermore, the nanoparticles get deposited on the heater surface and alter the profile of active nucleation sites. The roles of interfacial forces were altered in nanofluids rather than in pure liquids due to the

spontaneous phenomenon of nanoparticle adsorption at bubble interfaces which causes formation of smaller bubbles in nanofluids [146].

The data of bubble detachment time for water and nanofluids at different heat fluxes has been plotted in Fig. 6.11. Bubble detachment time refers to the time from the beginning of bubble growth to the moment when the bubble departs from the heating surface. It is found that the departure time decreases with increase in nanoparticle volume concentration of nanofluids. This means the increasing of nanoparticle volume concentration may enhance the intensity of nanofluids boiling heat transfer. In case of water boiling, bubble departure was delayed owing tobubble coalescence and bubble detachment time increased giving rise to formation of larger bubbles. But with nanofluids, bubble detachment time was shorter and the bubbles get lifted off from the heater surface within a short span. The reason may be attributed to modified suface characteristics due to deposition of nanoparicles.

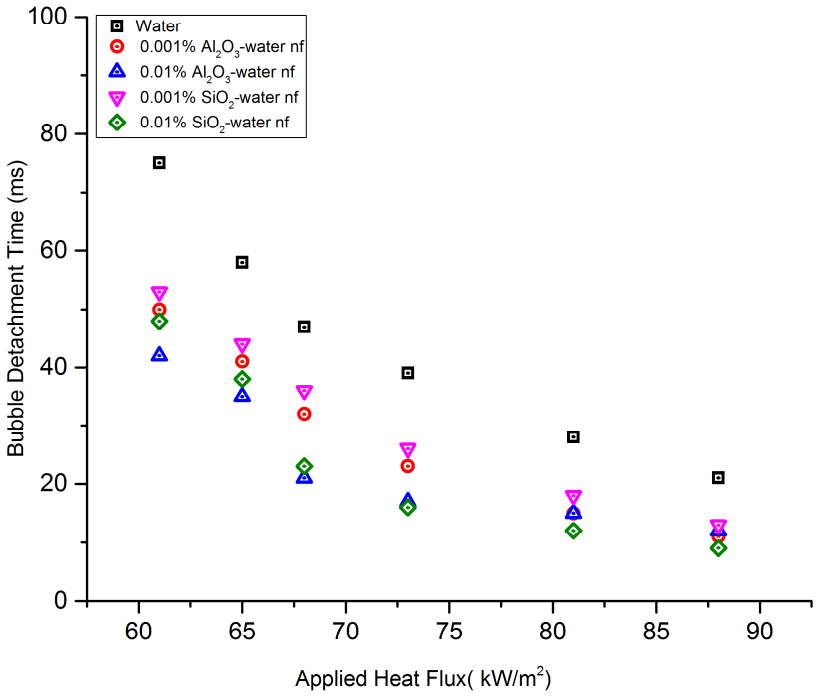

Fig. 6.11 Effect of heat flux on the bubble detachment time

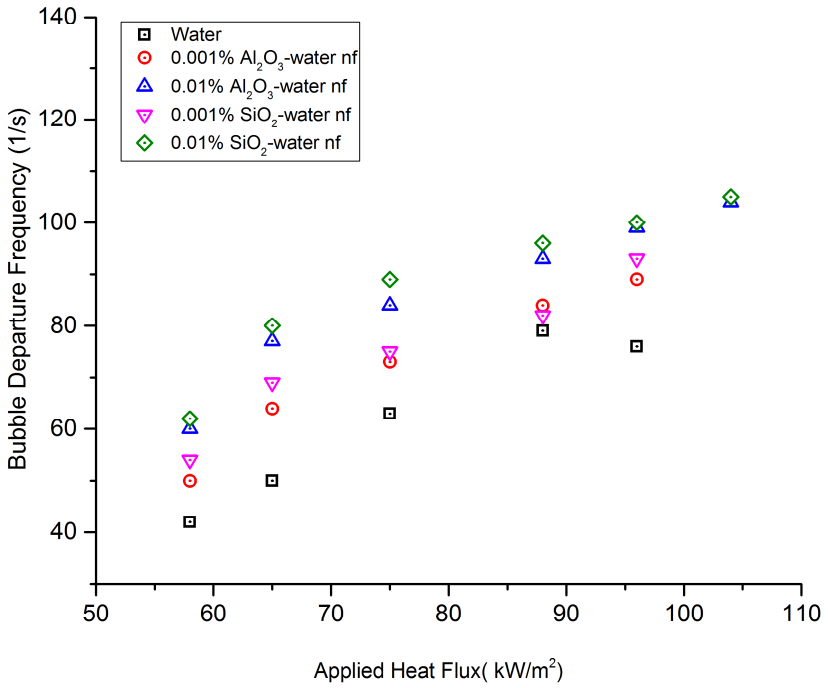

Fig. 6.12 Effect of heat flux on the bubble departure frequency

The data of bubble departure frequency for water and nanofluids at different heat fluxes has been plotted in Fig. 6.12. Bubble departure frequency is defined as the inverse of the time period between two consecutive bubble departures. The total time between two consecutive bubble departures include bubble growth time (t_g) and waiting time (t_w). The growth time is the time interval between the bubble nucleation and departure after growing at the nucleation site. The waiting time corresponds to the time from departure of the first bubble till a next bubble appears at the site. The bubble departure frequency is expressed as

$$f_d = \frac{1}{t_g + t_w} \tag{6.1}$$

It has been observed that, with increasing heat flux, evaporation rate increases and the number of bubbles departing per unit time increases. Hence, waiting period significantly

decreases with increasing heat flux for both water and nanofluids. Bubble growth period also slightly decreases with increasing heat flux. Both of these lead to higher departure frequency at higher heat flux for water and nanofluids. However, at very high heat flux ($\sim$ 100 kW/m^2), departure frequency decreases for water. The reason may be attributed to delayed bubble departure owing to bubble coalescence and bubble detachment time increased giving rise to lesser bubble departure frequency.

6.4 Flow Pattern Transition

In this section, the transition from bubbly flow to churn flow has been presented for water and nanofluids. The churn flow exhibited two phase oscillation and the amplitude of oscillation was more in water. Large, irregular bubbles occupied the test column leading to vigorous vapor jump in water. The vapor tried to push the liquid in downward direction whereas the liquid which was supplied from inlet tried to move upward causing chaotic movement and eventually two phase oscillation. The oscillation was caused by the flow pattern transition between bubbly flow with spherical bubbles and churn flow with large, elongated irregular bubbles as shown in Fig. 6.13. These large, irregular bubbles occupy the test section and reduce the flow rate through the channel. Due to these oscillations, the heater surface was alternately covered by liquid and vapor. With further increase in heat flux, the wetting area decreases and formation of dry patch occurs. This may lead to local burn out of the heater surface which was prohibited to protect the heater. At this instant of chaotic movement of fluid, power supply was turned off.

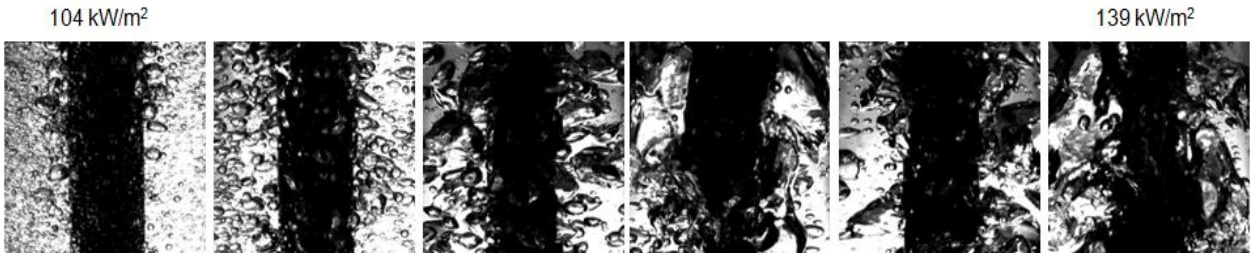

Water

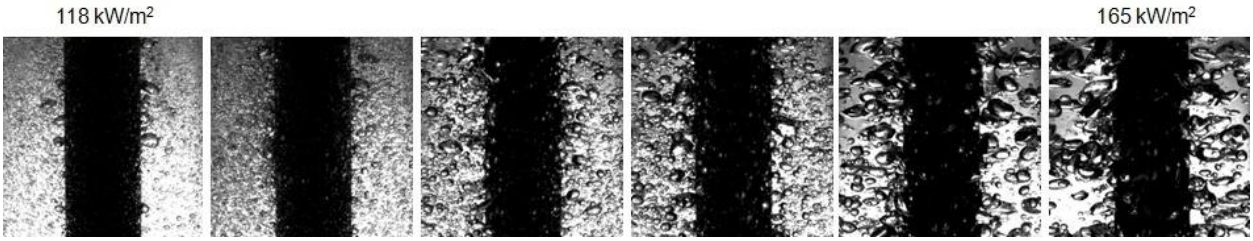

0.001% SiO_2/water nanofluid

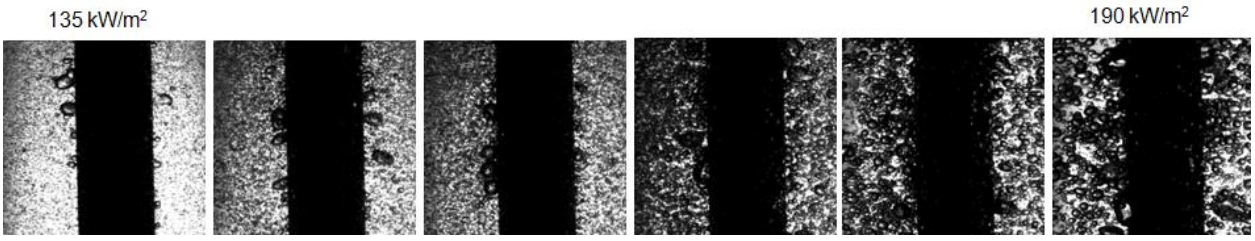

0.01% SiO_2/water nanofluid

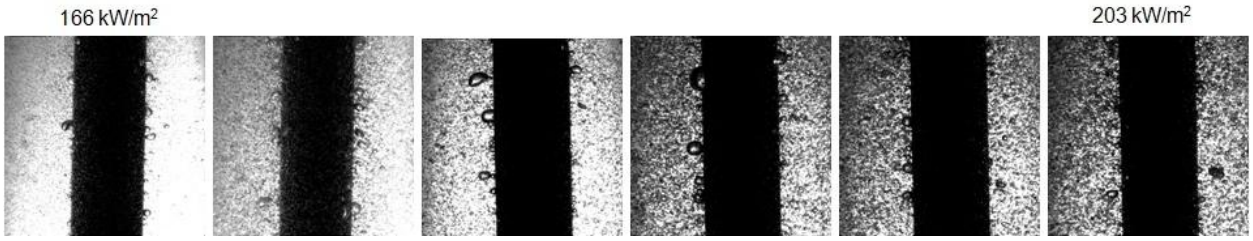

0.001% Al_2O_3/water nanofluid

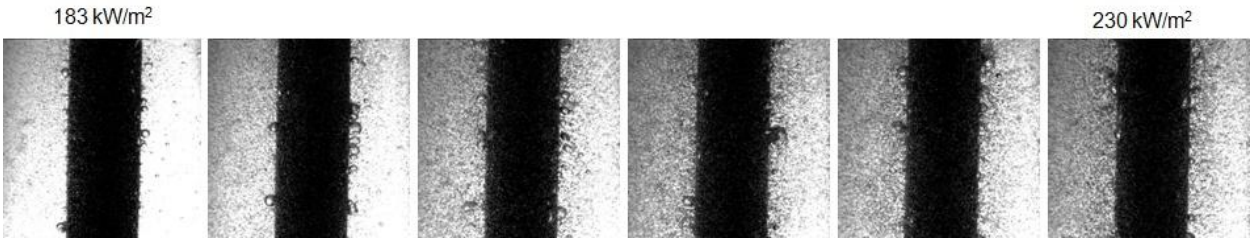

0.01% Al_2O_3/water nanofluid

Fig. 6.13 Flow Pattern Transition

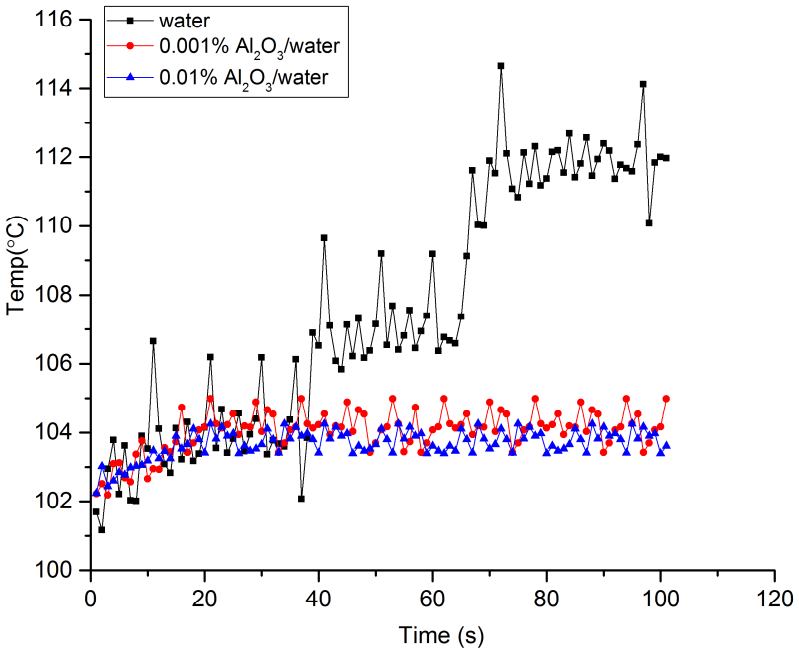

(a)

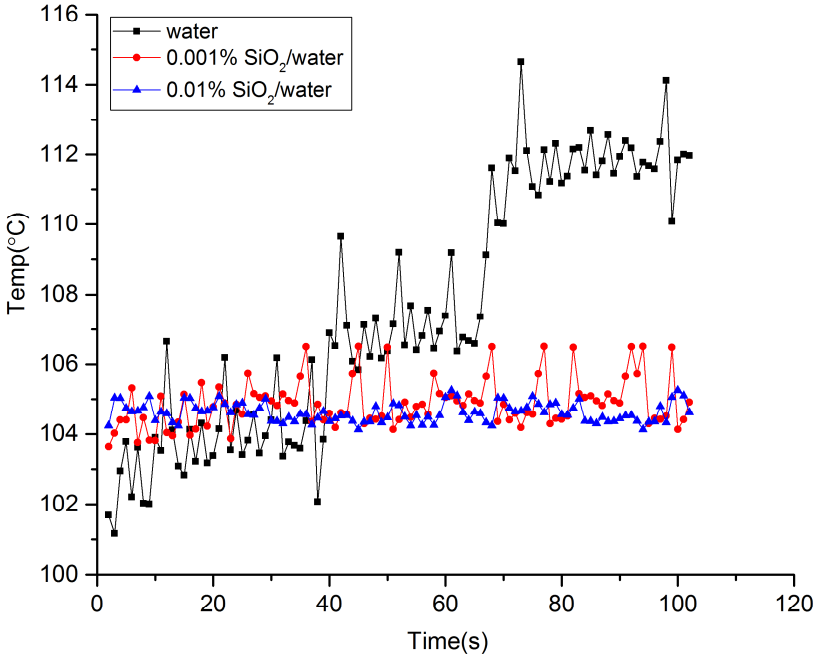

(b)

Fig. 6.14 Temperature Fluctuation during Flow Oscillation

(a) Water and Alumina Nanofluid (b) Water and Silica Nanofluid

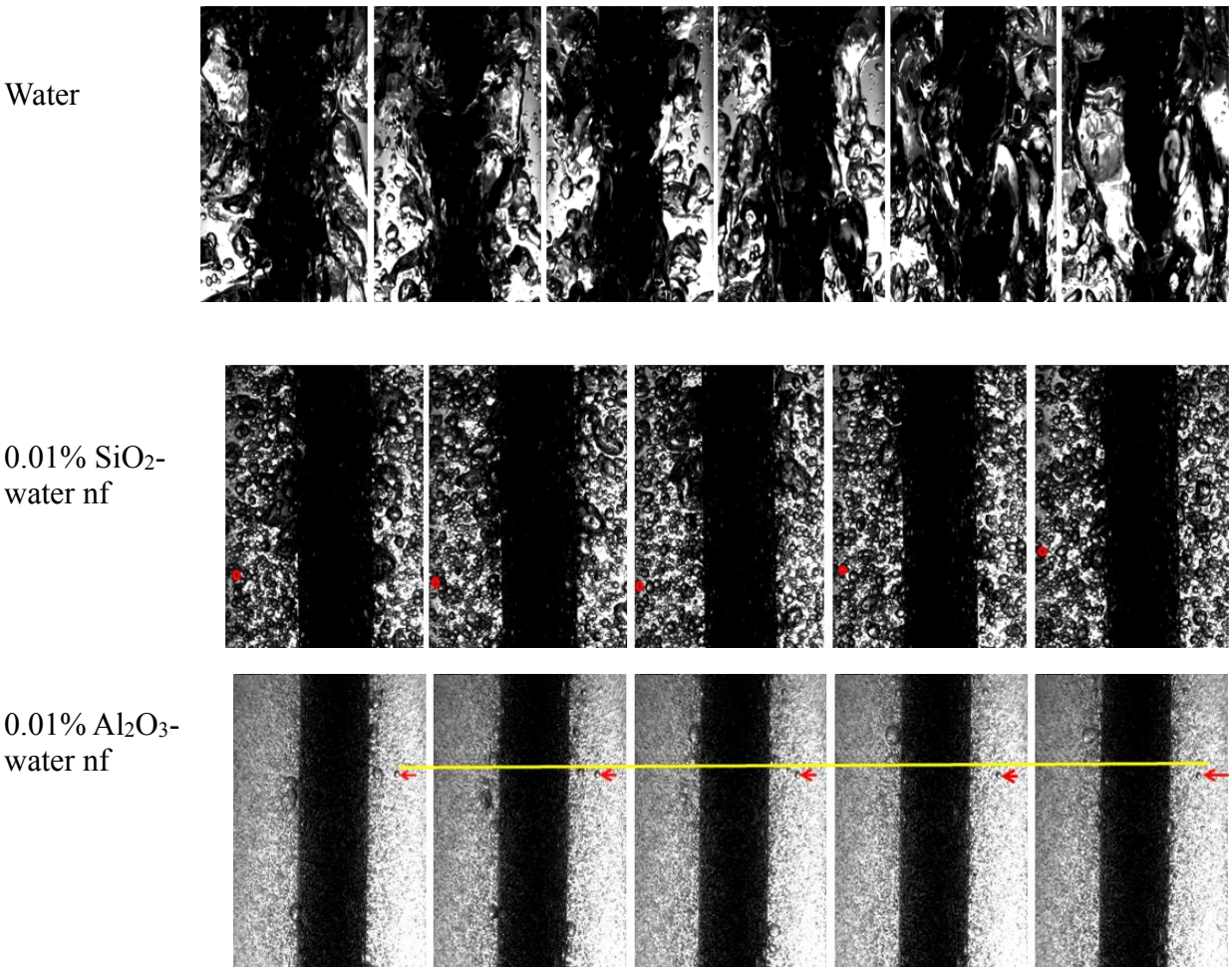

Fig. 6.15 Consecutive Images showing oscillation amplitude in water and nanofluids

As observed in high speed video, the flow pattern changed within a short span of time in pure water. With increasing heat flux, the bubbles merged with each other forming large bubbles which cover the heater surface by few centimeters. This causes temperature fluctuation on the heater surface which may lead to thermal shock on the heater surface. The temperature fluctuation during oscillation has been shown in Fig. 6.14. During water boiling, temperature fluctuation occurred over a range of 10-12°C, while the wall temperature was almost steady with a fluctuation of 2-6°C in nanofluids. The bubble size decreases with increase in concentration as well as varies according to type of nanoparticle dispersed in the fluid. The tiny bubbles suspended in the flow

generate less amount of vapor and reduce compressibility in the flow channel. The disturbance caused by miniature bubbles is smaller than caused by large irregular bubbles. This phenomenon suppress the oscillation and the extent of suppression is proportional to nanoparticle concentration. The amplitude of oscillation was less in nanofluids and the transition occurred very slowly. To give a clear picture, a single bubble has been marked and its location is identified during oscillation in Fig. 6.15. The presence of nanoparticles reduced the void fraction at a given heat flux and thereby suppress the oscillation.

6.5 Summary

Visualization studies on the flow boiling heat transfer of water and nanofluids (0.001%and 0.01% v/v) have been conducted. Bubble growth, departure and the flow pattern evolution during flow boiling have been investigated with the aid of high-speed photography. The test conditions were set under various thermal hydraulic conditions in order to study the effects of several parameters that affect the bubble dynamics. Results show that bubble size increased with increase in heat flux in both water and nanofluids, but the growth was more in pure water at higher heat flux resulting larger and irregular bubbles which initiated flow oscillation earlier than nanofluids. Under the same condition, the bubble in nanofluid departs from the heating surface earlier. The bubble size before the bubble departure is smaller for nanofluid than that for pure water.